INTERNATIONAL JOURNAL FOR NUMERICAL METHODS IN FLUIDS, VOL. 24, 563–578 (1997)

A MIXED GREEN ELEMENT FORMULATION FOR THE TRANSIENT BURGERS EQUATION

AKPOFURE E. TAIGBENU

Department of Civil Engineering, University of Benin, PMB 1154, Benin City, Nigeria

AND

OKEY O. ONYEJEKWE

Department of Civil Engineering, University of Durban-Westville, PB X54001, Durban 4000, South Africa

SUMMARY

The transient one-dimensional Burgers equation is solved by a mixed formulation of the Green element method (GEM) which is based essentially on the singular integral theory of the boundary element method (BEM). The GEM employs the fundamental solution of the term with the highest derivative to construct a system of discrete first-order non-linear equations in terms of the primary variable, the velocity, and its spatial derivative which are solved by a two-level generalized and a modified time discretization scheme and by the Newton–Raphson algorithm. We found that the two-level scheme with a weight of 0·67 and the modified fully implicit scheme with a weight of 1·5 offered some marginal gains in accuracy. Three numerical examples which cover a wide range of flow regimes are used to demonstrate the capabilities of the present formulation. Improvement of the present formulation over an earlier BE formulation which uses a linearized operator of the differential equation is demonstrated. © 1997 by John Wiley & Sons, Ltd.

KEY WORDS: Burgers equation; Green element

1. INTRODUCTION

The Burgers equation, which represents a combination of viscous and inertial components, is a quasi-linear partial differential equation capable of exhibiting some very unique phenomena. When the inertial term is dominant, its solution resembles that of the kinetic wave equation which displays a propagating wave front and boundary layers. On the other hand, viscous dominance causes dissipation and smearing of the solution wave front.

The primary mathematical difficulty involved in the solution of the Burgers equation arises from the sudden change in the solution profile over small regions. Research interests over the years have dwelt on accurately representing the scalar values in these areas of rapid change. The greater number of analytical solutions, which are summarized by Benton and Platzman,[1] has been obtained for infinite domains by the Cole–Hopf transformation,[2,3] which simplifies the non-linear Burgers equation to a linear diffusion equation.

The large array of numerical solutions of the Burgers equation has been based on various versions of the finite difference and finite element methods (FDM and FEM). Fletcher[4] carried out a thorough treatment of various Galerkin FE formulations and applied them to the propagating shock problem. His results and conclusions suggest no clear-cut advantage of his finite element formulation over

CCC 0271–2091/97/060563–16 $17.50
© 1997 by John Wiley & Sons, Ltd.
Received May 1995
Revised June 1996

other traditional methods such as the finite difference technique. Varoglu and Finn[5] adopted a finite element approach which used isoparametric space–time elements and incorporated the method of characteristics. their method, which is actually an improvement on earlier work by Bonnerot and Jamet,[6] yielded good results for a wide range of flow parameters. Epperson[7] applied a linear semigroup linearization to solve non-linear parabolic equations. In a subsequent work[8] he used a modified version of the same technique to decouple the non-linear convective term of a parabolic partial differential equation to obtain a very accurate prediction of the scalar profile. A more recent work based on the finite analytic method has been that of Onyejekwe,[9] who used an adaptive grid algorithm to resolve the steep profiles of the dependent variable. Applying the boundary element method (BEM), Kakuda and Tosaka[10] used the free space Green function for the linearized differential operator and solved the integral equations in each subdomain.

Here we improve on the BE solution of Kakuda and Tosaka[10] by an approach, referred to as the Green element method (GEM), which derives its fundamental solution from the term with the highest derivative so that the non-linear inertial or convective term is treated more accurately. The improvement in the accuracy of the numerical solution is demonstrated with the first example. The successful application of the GEM to linear and non-linear differential operators,[11] which hitherto had proved difficult with the boundary element theory, provides the motivation for the current work. Three numerical flow problems governed by the Burgers equation are used to demonstrate the capabilities of the current formulation. The numerical results show that the GEM is capable of solving the Burgers equation for flow regimes which cover small and large values of the viscosity parameter.

2. GREEN ELEMENT FORMULATION

The partial differential equation that governs the non-linear fluid flow phenomenon of shocks or wave propagation, widely known as the Burgers equation, is given by

$$\nu \frac{\partial^2 u(x,t)}{\partial x^2} = u(x,t)\frac{\partial u(x,t)}{\partial x} + \frac{\partial u(x,t)}{\partial t} \quad \text{on } x_0 \leqslant x \leqslant x_L, \tag{1}$$

in which $\nu = 1/R_e$ is the reciprocal of the flow Reynolds number defined by appropriate length and velocity scales of the flow, x and t are the spatial and temporal independent variables respectively and $L = x_0 - x_L$ is the length of the flow domain. In addition to (1), boundary and initial data have to be prescribed for the problem to be well posed. The boundary conditions are either of a Dirichlet type which specifies the velocity,

$$u(x_0, t) = g_0(t), \qquad u(x_L, t) = g_L(t), \tag{2a}$$

or of a Neumann type which specifies the spatial derivative of the velocity,

$$\frac{\partial u(0,t)}{\partial x} = f_0(t), \qquad \frac{\partial u(L,t)}{\partial x} = f_L(t), \tag{2b}$$

or an appropriate combination of the two. The initial data specify the velocity at the initial time t_0:

$$u(x, t_0) = u_0, \quad x_0 \leqslant x \leqslant x_L. \tag{2c}$$

The Green element formulation is based on the Fredholm singular integral theory which employs the free space Green function of the term with the highest derivative or the 1D Laplace differential operator. By adopting this approach, we avoid linearizing the differential equation to enable us obtain

 © 1997 by John Wiley & Sons, Ltd.

the free space Green function for the problem. The free space Green function is obtained from the solution to

$$\frac{\mathrm{d}^2 G}{\mathrm{d}x^2} = \delta(x - x_i) \quad \text{on} \quad -\infty \leqslant x \leqslant \infty \tag{3}$$

in an infinite space in the x-dimension, where $\delta(x - x_i)$ is the Dirac delta function and x_i is commonly referred to as the source point. The general form of the solution to (3) is given by

$$G(x, x_i) = \frac{|x - x_i| + k}{2}, \tag{4a}$$

where k is an arbitrary constant. (Although k is an arbitrary constant, its value has to be judiciously chosen, otherwise some of the diagonal elements could have zero value. Certainly the value of k cannot be set to zero in our formulation, because this leads to the diagonal coefficients of the flux in the global matrix being zero, thereby producing a singular matrix.) We elect to set k to unity. With this value of k,

$$G(x, x_i) = \frac{|x - x_i| + 1}{2}. \tag{4b}$$

$G(x, x_i)$ is referred to as the free space Green function, the fundamental solution or the unit response function. It is the response of a system governed by (3) due to an instantaneous unit input. In one spatial dimension, Green's second identity is restated for two functions G and u which should be at least twice differentiable in space:

$$\int_{x_0}^{x_L} \left(\frac{\mathrm{d}^2 G}{\mathrm{d}x^2} - G \frac{\partial^2 u}{\partial x^2} \right) \mathrm{d}x = \left[u \frac{\mathrm{d}G}{\mathrm{d}x} - G \frac{\partial u}{\partial x} \right]_{x=x_0}^{x=x_L}. \tag{5}$$

Introducing (1) and (3) into (5) yields

$$\int_{x_0}^{x_L} \left[u\delta(x - x_i) - \nu^{-1} G \left(u \frac{\partial u}{\partial x} + \frac{\partial u}{\partial t} \right) \right] \mathrm{d}x = \left[u \frac{\mathrm{d}G}{\mathrm{d}x} - G \frac{\partial u}{\partial x} \right]_{x=x_0}^{x=x_L}, \tag{6a}$$

which is simplified further to

$$-\lambda u(x_i, t) + \left[u \frac{\mathrm{d}G}{\mathrm{d}x} - G \frac{\partial u}{\partial x} \right]_{x=x_0}^{x=x_L} + \nu^{-1} \int_{x_0}^{x-L} G \left(u \frac{\partial u}{\partial x} + \frac{\partial u}{\partial t} \right) \mathrm{d}x = 0, \tag{6b}$$

where λ takes the value of unity if x_i is within the interval $x_0 < x < x_L$ and $\lambda = \frac{1}{2}$ if x_i is at the end points of the flow length.

The integral representation of (1), given by (6b), is discretized by piecewise linear segments or elements over which a distribution of the primary variable u and its spatial derivatives $\partial u/\partial x$ is prescribed. We have employed a linear distribution of those quantities over each element. By following this approach, the numerical solution comprises two quantities at each node, i.e. u and $\partial u/\partial x$, which is why it is a mixed formulation. The advantage of such a mixed formulation is that the primary variable u and its spatial derivatives are approximated to the same order of accuracy. In other words, u and $\partial u/\partial x$ have C° continuity. This approach is in contrast with those of other numerical methods where the flux is treated as a secondary variable that is obtained from the primary variable by numerical differentiation, thereby reducing by one order the accuracy of the spatial derivative of

© 1997 by John Wiley & Sons, Ltd.

the primary variable. The flow domain is discretized into N elements and in each element u and $\partial u/\partial x$ are approximated by linear interpolation functions in space,

$$u(x,t) = \Omega_1^e u_1^e(t) + \Omega_2^e u_2^e(t), \qquad \frac{\partial u(x,t)}{\partial x} = \Omega_1^e \frac{\partial u_1^e}{\partial x}(t) + \Omega_2^e \frac{\partial u_2^e}{\partial x}(t), \tag{7}$$

in which the superscript e denotes a typical element as shown in Figure 1 and the interpolating functions are $\Omega_1^e(\zeta) = 1 - \zeta$ and $\Omega_2^e(\zeta) = \zeta$, where $\zeta = (x - x_1^e)/l^e$, $0 \leqslant \zeta \leqslant 1$, is a local co-ordinate that has its origin at node 1 of the eth element and l^e is the length of the element. Within this typical element the integral equation (6b) is

$$-\lambda^e u(x_i^e, t) + \left[u\frac{\mathrm{d}G}{\mathrm{d}x} - G\frac{\partial u}{\partial x} \right]_{x=x_1^e}^{x=x_2^e} + v^{-1} \int_{x_1^e}^{x_2^e} G\left(u\frac{\partial u}{\partial x} + \frac{\partial u}{\partial t} \right) \mathrm{d}x = 0. \tag{8}$$

Introducing (7) into (8) and making use of the fact that $\mathrm{d}G(x, x_i)/\mathrm{d}x = [H(x - x_i) - H(x_i - x)]/2$, where H is the Heaviside function, equation (8) becomes

$$\frac{1}{2}\left\{ v\left(-u_1^e + u_2^e + \frac{\partial u_1^e}{\partial x} - (l^e + 1)\frac{\partial u_2^e}{\partial x} \right) + l^e \int_0^1 (l^e\zeta + 1)\left[(\Omega_1^e u_1^e + \Omega_2^e)\left(\Omega_1^e \frac{\partial u_1^e}{\partial x} + \Omega_2^e \frac{\partial u_2^e}{\partial x} \right) + \Omega_1^e \frac{\mathrm{d}u_1^e}{\mathrm{d}t} + \Omega_2^e \frac{\mathrm{d}u_2^e}{\mathrm{d}t} \right] \mathrm{d}\zeta \right\} = 0 \tag{9a}$$

when the source node is at node 1 of the element and

$$\frac{1}{2}\left\{ v\left(u_1^e - u_2^e + (l^e + 1)\frac{\partial u_1^e}{\partial x} - \frac{\partial u_2^e}{\partial x} \right) + l^e \int_0^1 [l^e(1 - \zeta) + 1]\left[(\Omega_1^e u_1^e + \Omega_2^e u_2^e)\left(\Omega_1^e \frac{\partial u_1^e}{\partial x} + \Omega_2^e \frac{\partial u_2^e}{\partial x} \right) + \Omega_1^e \frac{\mathrm{d}u_1^e}{\mathrm{d}t} + \Omega_2^e \frac{\mathrm{d}u_2^e}{\mathrm{d}t} \right] \mathrm{d}\zeta \right\} = 0 \tag{9b}$$

when the source node is at node 2 of the element. Equation (9a) and (9b) are combined and expressed in matrix form as

$$v\left(R_{ij}^e u_j^e + L_{ij}^e \frac{\partial u_j^e}{\partial x} \right) + V_{ijl}^e u_j^e \frac{\partial u_l^e}{\partial x} + T_{ij}^e \frac{\mathrm{d}u_j^e}{\mathrm{d}t} = 0, \quad i, j, l = 1, 2, \tag{10}$$

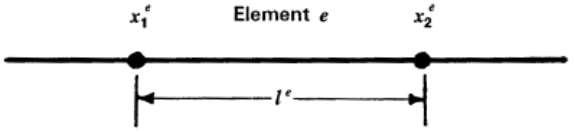

Figure 1. Definition sketch for linear 1D element

 © 1997 by John Wiley & Sons, Ltd.

in which the elemental matrices are

$$R_{ij}^e = \begin{bmatrix} -1 & 1 \\ 1 & -1 \end{bmatrix}, \quad i,j = 1,2, \tag{11a}$$

$$L_{ij}^e = \begin{bmatrix} 1 & -(1+l^e) \\ 1+l^e & -1 \end{bmatrix}, \quad i,j = 1,2, \tag{11b}$$

$$T_{ij}^e = l^e \int_0^1 \Omega_j^e(\zeta)(l^e|\zeta - \zeta_i| + 1)\mathrm{d}\zeta = \frac{l^e}{6}\begin{bmatrix} 3+l^e & 3+2l^e \\ 3+2l^e & 3+2l^e \end{bmatrix}, \quad i,j = 1,2, \tag{11c}$$

$$\begin{gathered} V_{ijl}^e = l^e \int_0^1 \Omega_j^e(\zeta)\Omega_l^e(\zeta)(l^e|\zeta - \zeta_i| + 1)\mathrm{d}\zeta, \quad 1,j,l = 1,2, \\ V_{1jl}^e = \frac{l^e}{12}\begin{bmatrix} 4+l^e & 2+l^e \\ 2+l^e & 4+3l^e \end{bmatrix}, \qquad V_{2jl}^e = \frac{l^e}{12}\begin{bmatrix} 4+3l^e & 2+l^e \\ 2+l^e & 4+l^e \end{bmatrix}. \end{gathered} \tag{11d}$$

Equation (10) is a system of non-linear first-order differential equations in time which can be solved for u and $\partial u/\partial x$ at the nodes by first employing an appropriate approximation of the temporal derivatives and then a non-linear solution algorithm. We elect to use the two-level time discretization scheme that approximates the temporal derivative at $t = t_{m+\alpha} = t_m + \alpha\Delta t$ so that equation (10) becomes

$$\begin{aligned} &\alpha\left[v\left(R_{ij}^e u_{j,m+1}^e + L_{ij}^e \frac{\partial u_{j,m+1}^e}{\partial x}\right) + V_{ijl}^e u_{j,m+1}^e \frac{\partial u_{l,m+1}^e}{\partial x}\right] \\ &\quad + (1-\alpha)\left[v\left(R_{ij}^e u_{j,m}^e + L_{ij}^e \frac{\partial u_{j,m}^e}{\partial x}\right) + V_{ijl}^e u_{j,m}^e \frac{\partial u_{l,m}^e}{\partial x}\right] + T_{ij}^e\left(\frac{1}{\Delta t}(u_{j,m+1}^e - u_{j,m}^e)\right) = 0, \\ &\qquad\qquad i,j,l = 1,2, \quad 0 \leqslant \alpha \leqslant 1, \end{aligned} \tag{12}$$

in which α is a time-weighting factor, the subscripts $m+1$ and m denote the current and previous time levels respectively and $\Delta t = t_{m+1} - t_m$ is the time step. We also elect to use a modified fully implicit scheme that approximates the temporal derivative at t_{m+1} as

$$\left.\frac{\mathrm{d}u_j^e}{\mathrm{d}t}\right|_{t=t_{m+1}} = \frac{\mathrm{d}u_{j,m+1}^e}{\mathrm{d}t} \approx \frac{\alpha}{\Delta t}(u_{j,m+1}^e - u_{j,m}^e) + (1-\alpha)\frac{\mathrm{d}u_{j,m}^e}{\mathrm{d}t}, \quad 1 \leqslant \alpha \leqslant 2, \tag{13}$$

so that equation (10) becomes

$$\begin{aligned} &v\left(R_{ij}^e u_{j,m+1}^e + L_{ij}^e \frac{\partial u_{j,m+1}^e}{\partial x}\right) + V_{ijl}^e u_{j,m+1}^e \frac{\partial u_{l,m+1}^e}{\partial x} \\ &\quad + T_{ij}^e\left(\frac{\alpha}{\Delta t}(u_{j,m+1}^e - u_{j,m}^e) + (1-\alpha)\frac{\mathrm{d}u_{j,m}^e}{\mathrm{d}t}\right) = 0, \quad i,j,l = 1,2, \quad 1 \leqslant \alpha \leqslant 2. \end{aligned} \tag{14}$$

The Newton–Raphson (N–R) algorithm is used to simplify the system of non-linear equations. The N–RE algorithm is introduced into both time discretization schemes of the GEM, equation (12) and (14). In the usual way of implementing the algorithm, a solution $[u_{j,m+1}^{e,k}, \phi_{j,m+1}^{e,k}]^{\mathrm{T}}$ is first proposed for both equations and updated by

$$[u_{j,m+1}^{e,k+1}, \phi_{j,m+1}^{e,k+1}]^{\mathrm{T}} = [u_{j,m+1}^{e,k}, \phi_{j,m+1}^{e,k}]^{\mathrm{T}} + [\Delta u_{j,m+1}^{e,k+1}, \Delta\phi_{j,m+1}^{e,k+1}]^{\mathrm{T}}, \tag{15}$$

© 1997 by John Wiley & Sons, Ltd.

where $\phi = \partial u/\partial x$, the superscript T denotes vector transposition, k and $k+1$ denote the previous and current iteration values respectively and the increment given by the second term on the right-hand side is obtained from the matrix equation

$$J^{e,k}_{ij,m+1}\begin{pmatrix}\Delta u^{e,k+1}_{j,m+1}\\ \Delta\phi^{e,k+1}_{j,m+1}\end{pmatrix} = -E_i|^{e,k}_{j,m+1}. \tag{16}$$

In (16) the known vector E_i is the quantity on the left-hand side of either (12) or (14), with values of u and ϕ evaluated at the current time t_{m+1} but at the previous iteration k, and the Jacobian $J^{e,k}_{ij,m+1}$ takes the form

$$J^{e,k}_{ij,m+1} = \begin{pmatrix}\alpha(vR^e_{ij} + V^e_{ijl}\phi^{e,k}_{l,m+1}) + \dfrac{1}{\Delta t}T^e_{ij}\\ \alpha(vL^e_{ij} + V^e_{ijl}u^{e,k}_{l,m+1})\end{pmatrix}, \quad 0 \leqslant \alpha \leqslant 1, \tag{17}$$

For the generalized two-level scheme and

$$J^{e,k}_{ij,m+1} = \begin{pmatrix}vR^e_{ij} + V^e_{ijl}\phi^{e,k}_{l,m+1} + \dfrac{\alpha}{\Delta t}T^e_{ij}\\ vL^e_{ij} + V^e_{ijl}u^{e,k}_{l,m+1}\end{pmatrix}, \quad 1 \leqslant \alpha \leqslant 2, \tag{18}$$

For the modified fully implicit time discretization scheme. The final step is to assemble equation (16) for all N elements so that two degrees of freedom are maintained at each node and to implement the boundary and initial data given by (2). The resultant global equation is given by

$$A^k_{ij,m+1}\begin{pmatrix}\Delta u^{k+1}_{j,m+1}\\ \Delta\phi^{k+1}_{j,m+1}\end{pmatrix} = S^k_{i,m+1} \tag{19}$$

The global coefficient matrix is banded with a half-band width of two and with a row dimension that is twice the number of elements. Equation (19) is solved at each time step for as many number of times as necessary until convergence is achieved by

$$[\Delta u^{k+1}_{j,m+1}, \Delta\phi^{k+1}_{j,m+1}] \cdot [\Delta u^{k+1}_{j,m+1}, \Delta\phi^{k+1}_{j,m+1}]^{\mathrm{T}} < \varepsilon, \tag{20}$$

where ε is the convergence tolerance, a predetermined small quantity that reflects the level of accuracy that can be accommodated.

3. NUMERICAL EXAMPLES

Three numerical examples are used to demonstrate the capabilities of the current numerical model. The first two examples have analytic solutions which serve as bases for comparison with our numerical results, while the GEM solution for the third example is compared with that of the finite element method.

The first example is an initial sinusoidal wave which is allowed to propagate and diffuse within a confined flow domain in the x-direction. The problem has the boundary conditions

$$u(0,t) = 0, \qquad u(1,t) = 0, \qquad u(x,0) = \sin(\pi x). \tag{21}$$

The exact solution to this problem, in the form of an infinite series, has been provided by Cole.[2]

 © 1997 by John Wiley & Sons, Ltd.

The second example is an initial discontinuous wave form which is allowed to diffuse into a continuous wave form while at the same time being propagated in time along the x-direction. The initial and boundary conditions are given by

$$u(x,0)=\begin{cases}1, & x\leqslant 0,\\ 0, & x>0,\end{cases}\qquad u(-\infty k,t)=1,\qquad u(\infty,t)=0. \tag{22}$$

The exact solution, obtained by the Cole–Hopf transform, is given by Lighthill[12] as

$$u(x,t)=\frac{1}{1+\exp\left(\dfrac{x-t/2}{2v}\right)\operatorname{erfc}\left(\dfrac{-x}{2\sqrt{(vt)}}\right)\Big/\operatorname{erfc}\left(\dfrac{x-t}{2\sqrt{(vt)}}\right)} \tag{23}$$

The third example used in demonstrating the capabilities of the current numerical model, which has also been employed by other investigators,[5,10] has the initial and boundary conditions.

$$u(x,0)=\begin{cases}1, & x<5,\\ 6-x, & 5\leqslant x<6,\\ 0, & x>6,\end{cases}\qquad u(-100,t)=1,\qquad u(20,t)=0. \tag{24}$$

The time and spatial discretizations and other simulation data for the three numerical examples are summarized in Table I.

First numerical experiments were carried out to determine the optimum weighting factor of the two time discretization schemes that were used in approximating the temporal derivative (see equations (12) and (14)). The benchmark solutions of examples 1 and 2 and the range of values for the viscosity term in example 3 provided the basis for evaluating the accuracy of these time discretization schemes. In order to numerically determine the time scheme which most closely reproduces the exact solution, five values of the time-weighting factor were examined: $\alpha=0{\cdot}5$, 0·67, 1·0, 1·25 and 1·5. For this study the performance of the schemes is assessed by both the mean absolute deviation and the L-

Table I. Data for GEM simulations

Example	End point co-ordinates x_0	End point co-ordinates x_L	Flow parameter v	Time step Δt	Number of elements, N	Spatial discritization	Maximum number of iterations	Figure/table number(s)
1	0	1	1	0·01	20	Uniform	4	Table II
	0	1	10^1	0·01	40	Uniform	4	Table III, Figure 2
	0	1	10^2	0·01	100	Uniform	6	Table IV, Figure 3
	0	1	10^2	0·02	50	Non-uniform	6	Figure 6
	0	1	10^3	0·02	100	Non-uniform	6	Figure 7
	0	1	10^4	0·02		Non-uniform	6	Figure 8
2	1·5	2·5	0·025	100		Uniform	5	Figures 4, 9
	0·7	1·3	10^2	0·01	100	Uniform	6	Figures 5, 10
3	100	20	1	0·02	49	Non-uniform	4	Figure 11
	100	20	10^1	0·1	87	Non-uniform	5	Figure 12
	100	20	10^2	0·05	149	Non-uniform	6	Figure 13

© 1997 by John Wiley & Sons, Ltd.

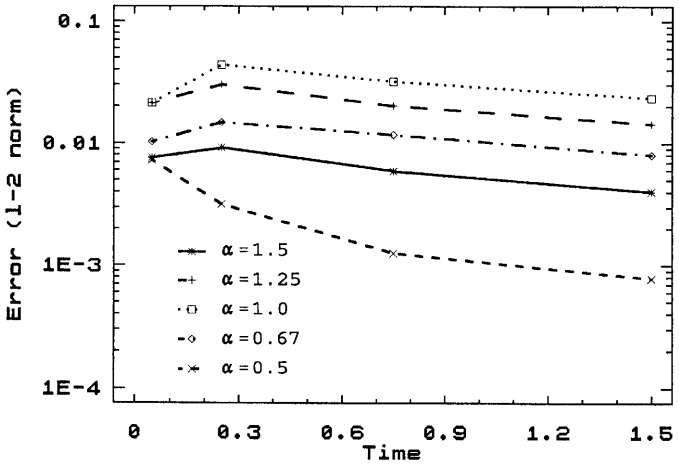

Figure 2. Error plots of time discretization schemes: example 1, $v = 10^{-1}$

2 norm, with each providing a method of determining quantitatively the error estimates between the numerical and analytic solutions. Graphical displays of error profiles at various times for $v = 10^{-1}$ and 10^{-2} for example 1 are presented in Figures 2 and 3, while those for example 2 are presented in Figures 4 and 5. Although the flow domain for example 2 is infinitely extensive, we have used finite domains, $-0{\cdot}7 \leqslant x \leqslant 1{\cdot}3$ for the case $v = 10^{-2}$ and $-1{\cdot}5 \leqslant x \leqslant 2{\cdot}5$ for the case $v = 10^{-1}$, so that the exact solutions at the end nodes satisfy the specified boundary conditions at $x = -\infty$ and ∞ throughout the simulation times. The performance of these time discretization schemes from Figures 2 through 5 is evaluated by determining which pair of weights from the two time schemes yields the best results. We observe that for example 1 (Figures 2 and 3), for both values of viscosity, $\alpha = 0{\cdot}5$ (two-level time schemes) and $\alpha = 1{\cdot}5$ (modified fully implicit) produced the best results. The worst results for the same figures were produced by $\alpha = 1{\cdot}0$ (two-level scheme) and $\alpha = 1{\cdot}25$ (modified fully implicit). Similarly, for example 2 (Figures 4 and 5) the best results were displayed by $\alpha = 0{\cdot}67$

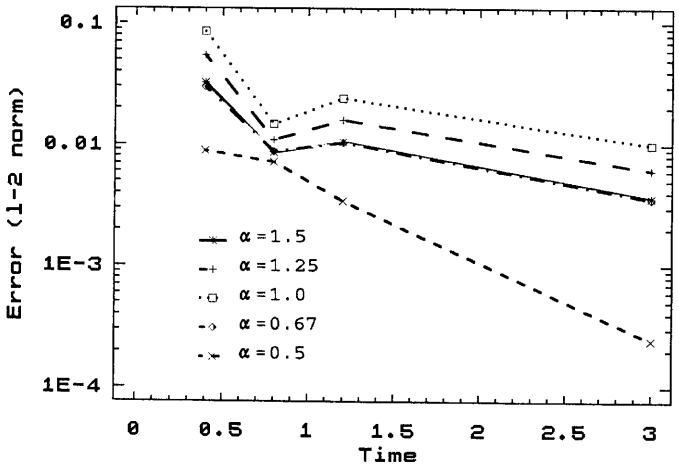

Figure 3. Error plots of time discretization schemes: example 1, $v = 10^{-2}$

 © 1997 by John Wiley & Sons, Ltd.

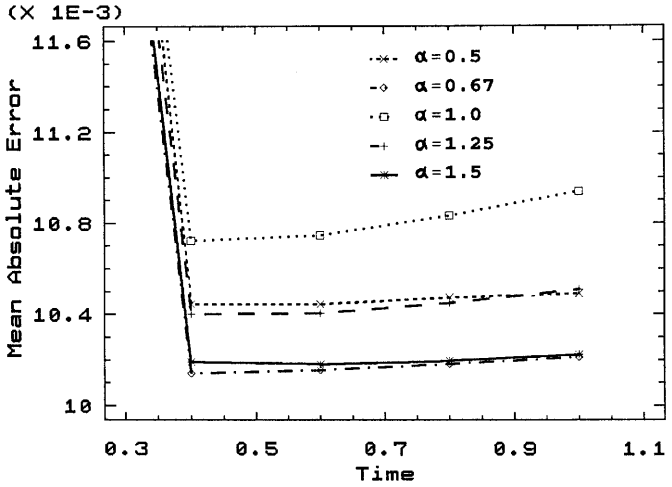

Figure 4. Error plots of time discretization schemes: example 2, $\nu = 10^{-1}$

(two-level scheme) and $\alpha = 1{\cdot}5$ (modified fully implicit) and the worst results by $\alpha = 0{\cdot}5$ (modified fully implicit) and $\alpha = 1{\cdot}0$ (two-level scheme).

Owing to the cluster of numerical results produced for $\alpha = 1{\cdot}25$ (fully implicit) and $\alpha = 0{\cdot}5$ of the two-level scheme (Figure 5), only those of the former are represented. In the same figure also there is an overlap of results obtained from $\alpha = 1{\cdot}5$ (fully implicit scheme) and $\alpha = 1{\cdot}0$ (two-level scheme), with the former giving results that are marginally better. Overall it should be observed that for cases where a pair of error profiles or appears very close (Figures 3–5), it suggests that the two weights of different time schemes yield very close results. On the basis of the pair that yields the smallest error, the schemes with $\alpha = 1{\cdot}5$ (modified fully implicit) and $\alpha = 0{\cdot}7$ (two-level scheme) are recommended for approximating the temporal derivative in the Green element formulation.

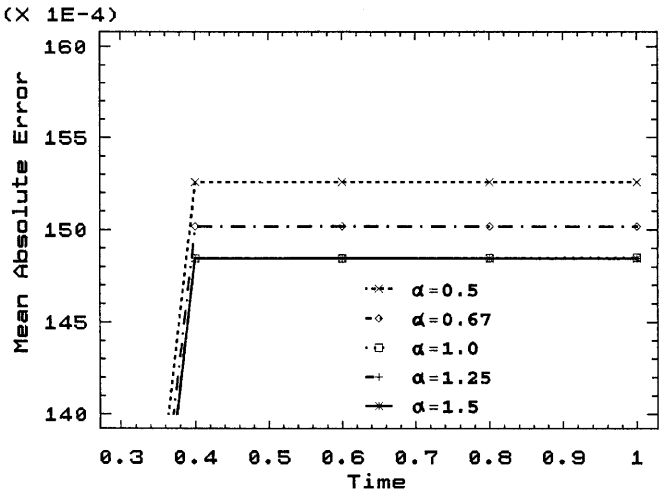

Figure 5. Error plots of time discretization schemes: example 2, $\nu = 10^{-2}$

© 1997 by John Wiley & Sons, Ltd.

Table II. Exact, BEM and GEM solutions for $v = 1$ for example 1

	$u(x, 0{\cdot}02)$			$u(x, 0{\cdot}04)$			$u(x, 0, 0{\cdot}10)$			$u(x, 0{\cdot}22)$		
x	BEM	GEM	Exact	BEM	GEM	Exact	BEM	GEM	Exact	BEM	GEM	Exact
0·00	0·00000	0·00000	0·00000	0·00000	0·00000	0·00000	0·000	0·00000	0·00000	0·00000	0·00000	0·00000
0·10	0·24617	0·24335	0·24369	0·19995	0·19664	0·19700	0·11215	0·10924	0·10954	0·03618	0·03433	0·03454
0·20	0·47052	0·46558	0·46618	0·38295	0·37698	0·37763	0·21473	0·20922	0·20979	0·06900	0·06547	0·06586
0·30	0·65261	0·64673	0·64742	0·53284	0·52532	0·52613	0·29865	0·29110	0·29190	0·09536	0·09046	0·09101
0·40	0·77477	0·76926	0·76988	0·63519	0·62743	0·62828	0·35579	0·34696	0·34792	0·11269	0·10686	0·10751
0·50	0·82376	0·81966	0·82010	0·67173	0·67248	0·37975	0·37054	0·37158	0·11917	0·11296	0·11367	
0·60	0·79242	0·79017	0·79039	0·65585	0·65-79	0·65137	0·36672	0·35802	0·35905	0·11400	0·10802	0·10870
0·70	0·68118	0·68058	0·68064	0·56632	0·56315	0·56354	0·31635	0·30900	0·30991	0·09748	0·09234	0·09294
0·80	0·49912	0·49947	0·49943	0·41648	0·41487	0·41510	0·23245	0·22714	0·22782	0·07112	0·06736	0·06779
0·90	0·26386	0·26431	0·26427	0·22069	0·22010	0·22019	0·12310	0·12033	0·12069	0·03749	0·03550	0·03573
1·00	0·00000	0·00000	0·00000	0·00000	0·00000	0·00000	0·00000	0·00000	0·00000	0·00000	0·00000	0·00000
Error	$9{\cdot}69 \times 10^3$	$1{\cdot}26 \times 10^3$		$1{\cdot}40 \times 10^2$	$1{\cdot}74 \times 10^3$		$1{\cdot}83 \times 10^2$	$2{\cdot}35 \times 10^3$		$1{\cdot}23 \times 10^2$	$1{\cdot}58 \times 10^3$	

Table III. Exact, BEM and GEM solutions for $v = 10^1$ for example 1

	$u(x, 0{\cdot}05)$			$u(x, 0{\cdot}25)$			$u(x, 0, 0{\cdot}75)$			$u(x, 1{\cdot}5)$		
x	BEM	GEM	Exact	BEM	GEM	Exact	BEM	GEM	Exact	BEM	GEM	Exact
0·00	0·00000	0·00000	0·00000	0·00000	0·00000	0·00000	0·000	0·00000	0·00000	0·00000	0·00000	0·00000
0·10	0·26117	0·25847	0·25869	0·16327	0·16011	0·16026	0·08473	0·08340	0·08343	0·04413	0·04374	0·04375
0·20	0·50403	0·49976	0·50005	0·32173	0·31597	0·31623	0·16799	0·16547	0·16552	0·08650	0·08575	0·08573
0·30	0·71031	0·70630	0·70646	0·46995	0·46271	0·46300	0·24788	0·24442	0·24448	0·12498	0·12393	0·12394
0·40	0·86200	0·85996	0·85990	0·60100	0·59388	0·59409	0·32129	0·31734	0·31738	0·15681	0·15554	0·15556
0·50	0·94186	0·94259	0·94237	0·70500	0·69997	0·70001	0·38277	0·37891	0·37892	0·17824	0·17687	0·17691
0·60	0·93473	0·93763	0·93743	0·76636	0·76551	0·76530	0·42229	0·41924	0·41922	0·18455	0·18319	0·18327
0·70	0·83003	0·83349	0·83343	0·75937	0·76412	0·76372	0·42256	0·42093	0·42093	0·17071	0·16951	0·16962
0·80	0·62643	0·62891	0·62896	0·64470	0·65411	0·65373	0·35900	0·35896	0·13332	0·13242	0·13253	0·13253
0·90	0·33825	0·33932	0·33926	0·38421	0·39274	0·39259	0·21298	0·21312	0·07365	0·07316	0·07323	0·07323
1·00	0·00000	0·00000	0·00000	0·00000	0·00000	0·00000	0·00000	0·00000	0·00000	0·00000	0·00000	0·00000
Error	$8{\cdot}23 \times 10^3$	$5{\cdot}10 \times 10^4$		$1{\cdot}82 \times 10^2$	$7{\cdot}69 \times 10^4$		$7{\cdot}87 \times 10^3$	$1{\cdot}87 \times 10^4$		$2{\cdot}96 \times 10^3$	$1{\cdot}95 \times 10^4$	

© 1997 by John Wiley & Sons, Ltd.

Table IV. Exact, BEM and GEM solutions for $v = 10^2$ for example 1

	$u(x, 0{\cdot}4)$			$u(x, 0{\cdot}8)$			$u(x, 0, 1{\cdot}20)$			$u(x, 3{\cdot}0)$		
x	BEM	GEM	Exact	BEM	GEM	Exact	BEM	GEM	Exact	BEM	GEM	Exact
0·00	0·00000	0·00000	0·00000	0·00000	0·00000	0·00000	0·000	0·00000	0·00000	0·00000	0·00000	0·00000
0·20	0·27628	0·27449	0·27452	0·17854	0·17734	0·17736	0·131091	0·13092	0·06036	0·06009	0·06009	
0·40	0·54060	0·53788	0·53792	0·35501	0·35279	0·35282	0·26285	0·26126	0·26128	0·12068	0·12016	0·12016
0·60	0·77506	0·77347	0·77345	0·52677	0·52398	0·52401	0·39264	0·39041	0·39044	0·18095	0·18017	0·18018
0·80	0·93765	0·94117	0·94100	0·68959	0·68708	0·68708	0·52012	0·51750	0·51753	0·23906	0·23867	0·23863
0·90	0·94407	0·95277	0·94891	0·76447	0·76311	0·76295	0·57950	0·57812	0·57781	0·23766	0·24183	0·24159
0·92	0·92675	0·93734	0·93655	0·77630	0·77645	0·77586	0·58466	0·58555	0·58472	0·22050	0·22636	0·22612
0·94	0·88895	0·90330	0·89998	0·77818	0·78320	0·78119	0·57336	0·57956	0·57779	0·18997	0·19708	0·19690
0·96	0·79386	0·81619	0·81227	0·73563	0·75388	0·74905	0·51253	0·52772	0·52524	0·14228	0·14919	0·14911
0·98	0·53348	0·66080	0·56583	0·52664	0·55927	0·55546	0·33294	0·35167	0·35061	0·07698	0·08139	0·08139
1·00	0·00000	0·00000	0·00000	0·00000	0·00000	0·00000	0·00000	0·00000	0·00000	0·00000	0·00000	0·00000
Error	$4{\cdot}06 \times 10^2$	$8{\cdot}20 \times 10^3$		$3{\cdot}23 \times 10^2$	$6{\cdot}50 \times 10^3$		$2{\cdot}26 \times 10^2$	$3{\cdot}35 \times 10^3$		$1{\cdot}27 \times 10^2$	$3{\cdot}95 \times 10^3$	

© 1997 by John Wiley & Sons, Ltd.

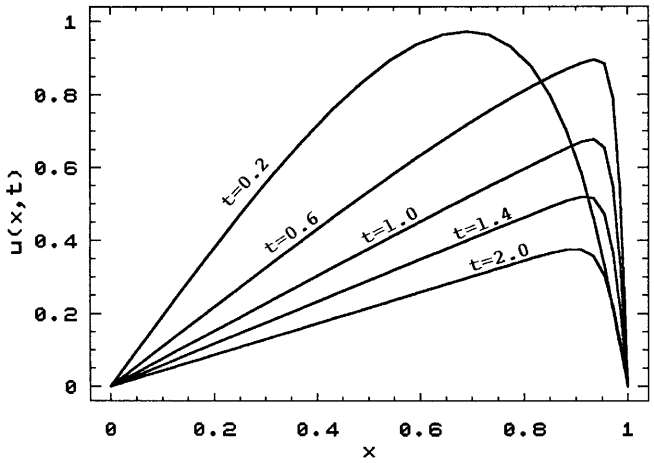

Figure 6. Gem solutions: example 1, $v = 10^{-2}$

Because the mixed Green element approach which we have adopted in this work is based on the same singular integral theory as the generalized BEM employed by Kakuda and Tosaka,[10] we have compared our solutions with their for example 1 at the times their solutions were tabulated. Our values of time and spatial discretizations and maximum number of iterations allowed at each time step are the same as theirs. Tables II–IV show both numerical solutions and exact solutions for values of $v = 1, 10^{-1}$ and 10^{-2}, together with the computed error estimates. The L-2 normal errors of the GEM are less than those of the generalized BEM formulation of Kakuda and Tosaka[10] at all times and for all Reynolds number values examined. These results show the loss of accuracy when the differential equation is linearized within the element, which has been avoided in the mixed GEM. Also, the simple nature of the fundamental solution employed in the mixed GEM formulation which

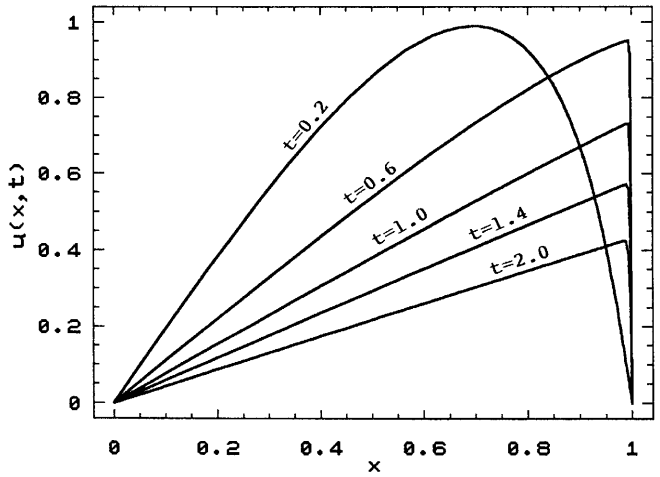

Figure 7. Gem solutions: example 1, $v = 10^{-3}$

 © 1997 by John Wiley & Sons, Ltd.

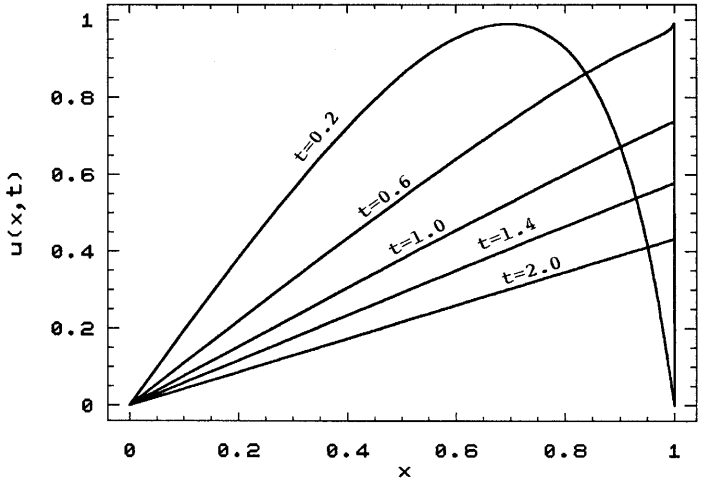

Figure 8. Gem solutions: example 1, $v = 10^{-4}$

made it possible for exact integration of the elemental integrals enhanced the accuracy of the numerical solutions, in contrast with the more complicated fundamental solution used by Kakuda and Tosaka[10] which required the use of quadrature techniques in evaluating the elemental integrals. This result further buttresses our earlier conclusions that a simple fundamental solution is preferable to a more complicated one even if it involves more domain integrations.[11,13–16]

The GEM solutions of the velocity profiles for $v = 10^{-2}, 10^{-3}$ and 10^{-4} for example 1 are presented at various times in Figures 6–8. These solutions compare quite favourably with the solutions of Varoglu and Finn[5] (not presented), which reflect the general behaviour of the solution in which a sharp front develops close to $x = 1$ at early times and decays later as a result of viscous action which becomes pronounced in the vicinity of large gradients of the velocity.

The exact and GEM solutions for $v = 10^{-1}$ and 10^{-2} for example 2 are presented in Figures 9 and 10. The sharp profile of the velocity for $v = 10_{-2}$ is reproduced by the GEM and it is significant to note that the numerical solutions do not exhibit any oscillations.

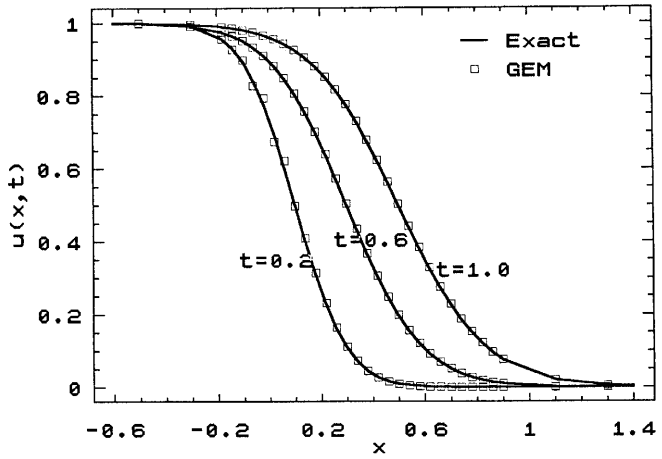

Figure 9. Exact and GEM solutions: example 2, $v = 10^{-1}$

© 1997 by John Wiley & Sons, Ltd.

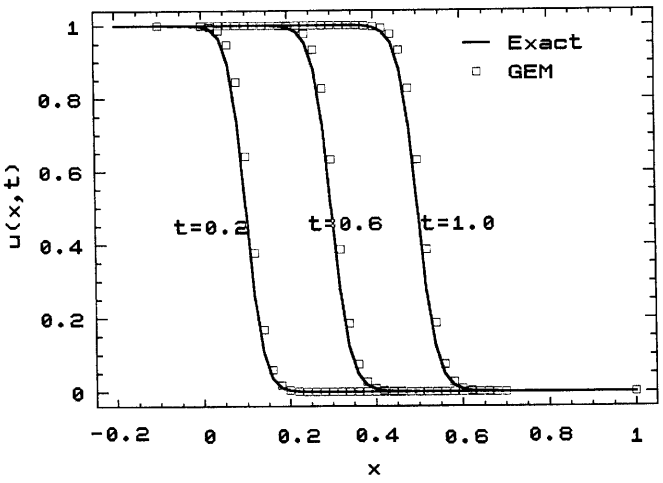

Figure 10. Exact and GEM solutions: example 2, $v = 10^{-2}$

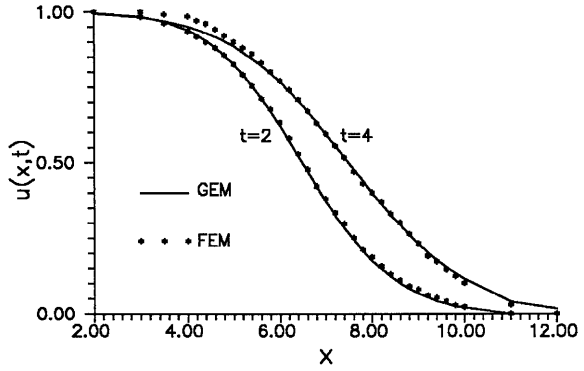

Figure 11. GEM and FEM solutions: example 3, $v = 10^{-1}$

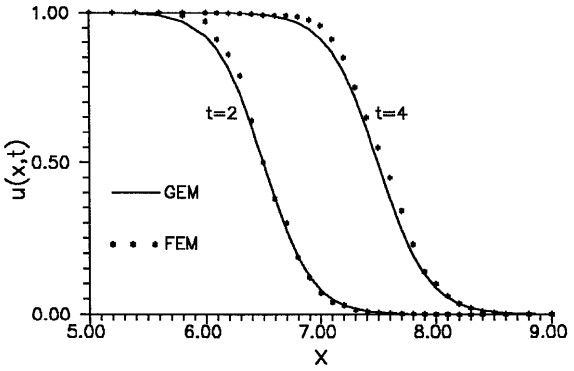

Figure 12. GEM and FEM solutions: example 3, $v = 10^{-1}$

 © 1997 by John Wiley & Sons, Ltd.

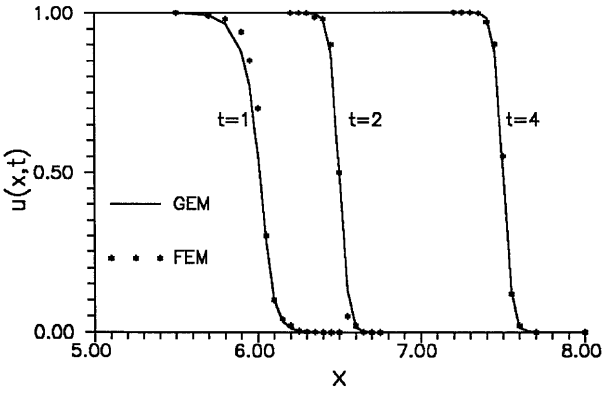

Figure 13. GEM and FEM solutions: example 3, $\nu = 10^{-2}$

A comparison of the GEM solutions with the finite element solutions of Varoglu and Finn[5] for $\nu = 1.10^{-1}$ and 10^{-2} for example 3 is presented in Figures 11–13. The steep velocity front of the propagating wave is reproduced for larger values of the Reynolds number by the GEM with no numerical dissipation and oscillation. Both numerical solutions are in good agreement.

4. CONCLUSIONS

A mixed formulation of the Green element method for the transient 1D Burgers equation has been presented. It follows earlier GEM formulations which had been applied to two-dimensional problems. By employing a simple kernel of the linear part of the differential equation, the singular theory of the BEM is implemented in an exact fashion within each element and then all elemental inputs are aggregated to form a discrete system of non-linear equations which are solved by the Newton–Raphson algorithm. Comparison of the two-level generalized and modified fully implicit discretization schemes shows that the scheme with $\alpha = 0{\cdot}67$ and the fully modified fully implicit scheme with $\alpha = 1{\cdot}5$ are marginally better in approximating the temporal derivative. The GEM solutions are superior to the generalized BEM solutions of Kakuda and Tosaka,[10] because the differential operator was not linearized in deriving the free space Green function. For the three numerical examples solved, the GEM gave acceptable solutions for a wide range of viscosity values using moderate sizes of time step and spatial increments. These results demonstrate one other useful computational strength of the Green element application to non-linear problems.

REFERENCES

1. E. R. Benton and G. W. Platzman, 'A table of solutions of the one-dimensional Burgers equation', *Q. Appl. Math.*, July, 195–212 (1972).
2. J. D. Cole, 'On a quasi-linear parabolic equation occurring in aerodynamics', *Q. Appl. Math.*, **23**, 225–236 (1951).
3. E. Hopf, 'The partial differential equation $u_t + uu_x = \mu u_{xx}$', *Commun. Pure Appl. Math.*, **3**, 201–230 (1950).
4. C. A. J. Fletcher, 'Burger's equation: a model for all reasons', in J. Noye (ed.) *Numerical Solutions of Partially Differential Equations*, North-Holland, Amsterdam, 1982, pp. 139–225.
5. E. Varoglu and W. D. L. Finn, 'Space–time finite elements incorporating characteristics for the Burgers' equations', *Int. j. numer. methods eng.*, **16**, 171–184 (1980).
6. R. Bonnerot and P. Jamet, 'A second order finite element method for the one-dimensional Stephan problem', *Int. j. numer. methods eng.*, **8**, 811–820 (1974).
7. J. Epperson, 'Semigroup linearization for nonlinear parabolic equations', *Number. Methods Partial Diff. Eq.*, **7**, 147–163 (1991).

© 1997 by John Wiley & Sons, Ltd.

8. J. Epperson, 'A kernel-based method for parabolic equations with nonlinear convection terms', *J. Comput. appl. Math.*, **36**, 275–288 (1991).
9. O. O. Onyejekwe, 'A finite analytic solution of Burgers' equation using a node moving algorithm;, *Proc. 34th Heat Transfer and Fluid Mechanics Conf.*, Sacramento, CA, 1990, pp. 245–261.
10. K. Kakuda and N. Tosaka, 'The generalized boundary element approach to Burgers' equation', *Int. j. numer. methods eng.*, **29**, 245–261 (1990).
11. A. E. Taigbenu, 'The Green element method', *Int. j. numer methods eng.*, **38**, 2241–2263.
12. M. J. Lighthill, 'Viscosity effects in sound waves of finite amplitude', in G. K. Batchelor and R. M. Davis (eds), *Surveys in Mechanics*, Cambridge University Press, Cambridge, 1956.
13. A. E. Taigbenu and J. A. Liggett, 'An integral formulation applied to the diffusion and Boussinesq equations', *Int. j. numer. methods eng.*, **23**, 1057–1079 (1986).
14. A. E. Taigbenu and J. A. Liggett, 'An integral solution for the diffusion–advection equation', *Water Resources Res.*, **22**. 1237–1246 (1986).
15. A. E. Taigbenu, 'A more efficient implementation of the boundary element theory', *Proc. 5th Int. Conf. on Boundary Element Technology (BETECH 90)*, Newark, DE, 1990, pp. 355–366.
16. O. O. Onyejekwe, 'A Green element description of mass transfer in reacing systems'. *Numer. Heat Transfer*, in press.

 © 1997 by John Wiley & Sons, Ltd.